Macromolecules

COMMUNICATION TO THE EDITOR

pubs.acs.org/Macromolecules

Nanoporous Polystyrene and Carbon Materials with Core−Shell Nanosphere-Interconnected Network Structure

Dingcai Wu,[*,†,‡] Chin Ming Hui,[†] Hongchen Dong,[†] Joanna Pietrasik,[§] Hyung Ju Ryu,[∥] Zhenghui Li,[‡] Mingjiang Zhong,[†] Hongkun He,[†] Eun Kyung Kim,[†] Mietek Jaroniec,[*,⊥] Tomasz Kowalewski,[*,†] and Krzysztof Matyjaszewski[*,†]

[†]Department of Chemistry, Carnegie Mellon University, 4400 Fifth Avenue, Pittsburgh, Pennsylvania 15213, United States

[‡]Materials Science Institute, Key Laboratory for Polymeric Composite and Functional Materials of Ministry of Education, School of Chemistry and Chemical Engineering, Sun Yat-sen University, Guangzhou 510275, P. R. China

[§]Institute of Polymer and Dye Technology, Technical University of Lodz, Stefanowskiego 12/16, 90 924 Lodz, Poland

[∥]Department of Materials Science and Engineering, Carnegie Mellon University, 5000 Forbes Avenue, Pittsburgh, Pennsylvania 15213, United States

[⊥]Department of Chemistry, Kent State University, Kent, Ohio 44242, United States

Supporting Information

Nanoporous polymers and their related carbon materials can incorporate many structural features, such as controllable pore shape and size, tunable pore surface chemistry, well-developed porosity, high surface area, good conductivity, and low bulk density.[1] Therefore, they find utility in many fields including adsorption, catalysis, separations, medicine, environmental, and energy-related applications.[1,2] Currently, there is an increased focus on the synthesis and examination of nanoporous materials with hierarchical nanostructures because they can exhibit the advantages of each of hierarchical pores with a synergistic effect and thus lead to fundamental breakthroughs that improve their properties in many applications.[3]

Nanostructured porous network (NPN) materials, with three-dimensionally (3D) continuous nanopores, are a very important class of porous materials. The high degree of pore connectivity can provide materials with good mass transport properties and improve material lifetime in applications where pore blockage is an issue, such as energy storage, adsorption, separations, and catalysis. However, since typical NPN materials are usually prepared using uncontrolled polymerizations, such as condensation or conventional free radical polymerization, their molecular and nanoscale structure cannot be well controlled. Thus, the networks prepared using current approaches are generally comprised of nanoparticulate network units which are poorly defined.[2i,3a,3d,4] This is well exemplified by the very typical NPN materials, organic aerogels based on phenolic monomers, and the corresponding carbon aerogels. Here, lack of accurate control of the condensation polymerization of phenolic monomers and of their supramolecular organization yields nanoparticulate network units with wide size distributions and ill-defined shapes.[2i,4]

Recently, we have developed a new class of NPN materials, in which the network units are microporous polystyrene nanoparticles cross-linked via formation of carbonyl (−CO−) bridges between polystyrene chains.[3a,d] This development resulted in the unique network-type microporosity and guaranteed the preservation of the nanostructure during carbonization, since carbonyl bridges ensure high cross-linking density and serve as a source of oxygen atoms.[3a,d] However, the network unit of such prepared nanonetworks still had the form of ill-defined solid nanoparticles[3a] and lacked any hierarchical structure.[3a,d]

Herein we describe a new strategy to address these shortcomings, which is based on the use of well-defined hairy nanoparticles as network precursors. Hairy nanoparticles, acting as core−shell network building blocks, were prepared by grafting polystyrene chains from the surface of silica nanoparticles using surface-initiated atom transfer radical polymerization (SI-ATRP),[5] followed by intra-/interparticle carbonyl cross-linking of polystyrene. The overall synthesis procedure is illustrated in Scheme 1.

This strategy has several significant advantages. First, it allows for the design and fabrication of network unit at a molecular level. Since the molecular structure of hairy nanoparticles can be tuned, the properties of the resulting NPN materials can be easily tailored. Another unique aspect of such prepared materials is derived from the core−shell structure of nanosphere network unit. The final NPNs contain three types of pores: (i) micropores induced by cross-linking of the hairy polystyrene shell, (ii) mesopores obtained by removal of sacrificial silica nanoparticle core, and (iii) meso-/macroporous network formed through interparticle cross-linking. Use of the unique, well-defined, core−shell network unit could afford the nanomaterials with advanced responsive properties and superior performance as storage/release matrices. Finally, the new synthetic approach described herein further exemplifies the use of controlled polymerizations, such as ATRP, for the preparation of nanoporous materials. In addition to the well-developed microporosity, the polystyrene-based framework opens the way to further functionalization and customization of surface chemistry.

The diameter of the bare SiO_2 nanoparticles, as measured by dynamic light scattering (DLS) analysis, was ∼18 nm, Figure 1, and ∼14 nm, according to the TEM image shown in Figure 2A. Slightly higher value of particle diameter obtained from DLS in comparison with TEM was, most likely, a result of their hydrodynamic

Received: June 11, 2011
Revised: July 3, 2011
Published: July 13, 2011

Scheme 1. Preparation Process of Novel NPN Polymer and Carbon Materials

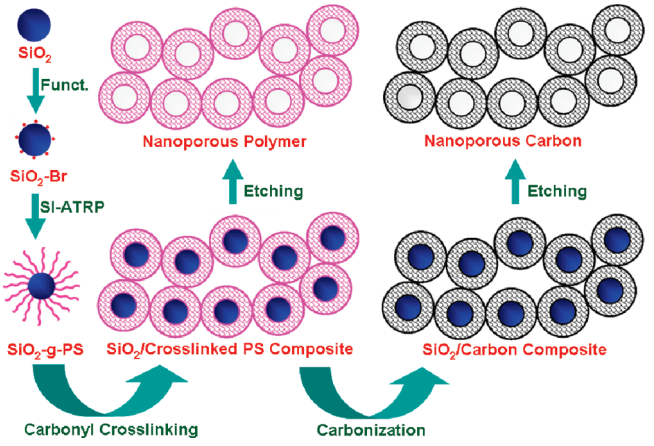

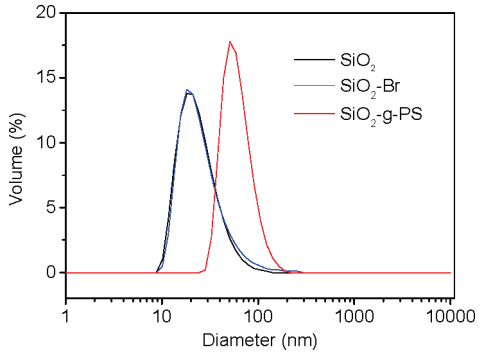

Figure 1. DLS size distributions for SiO_2, SiO_2—Br, and SiO_2-*g*-PS.

nature.[3d] The surface of the nanoparticles was functionalized by reaction with 1-(chlorodimethylsilyl)propyl 2-bromoisobutyrate to introduce Br-containing surface ATRP initiation sites.[5a] According to Figures 1 and 2B, the resulting SiO_2—Br nanoparticles functionalized with ATRP initiators have almost the same diameter as the parent SiO_2. Thus, the functionalization treatment essentially did not change the particle size. Subsequently, the SI-ATRP grafting of polystyrene from the SiO_2—Br nanoparticles was carried out, using the following molar ratio: styrene/SiO_2—Br/CuBr/$CuBr_2$/dNbpy = 1000/1/4/0.4/8.8 at 90 °C for 20.5 h. The purified PS-grafted SiO_2 (SiO_2-*g*-PS) powder dissolved in tetrahydrofuran (THF) at a concentration of 1 mg/mL had a narrow and unimodal size distribution with a maximum d = 51 nm, according to DLS (Figure 1). The PS was cleaved from the nanoparticles by etching with hydrofluoric acid (HF) and characterized by GPC. As shown in Figure S1, the cleaved PS had a narrow, unimodal peak with molecular weight M_n = 23 200 and M_w/M_n = 1.12, indicating an efficient SI-ATRP. The PS content of the SiO_2-*g*-PS nanoparticles, as measured by thermogravimetric analysis (Figure S2), was 69 wt %. Depending on whether one uses the diameter of silica nanoparticles determined by TEM or DLS (14 vs 18 nm), this polymer content translates into a relatively high grafting density of respectively 0.28 or 0.36 chains/nm^2.

The as-prepared SiO_2-*g*-PS nanoparticles were cast into a film from a chloroform solution of SiO_2-*g*-PS (concentration 10 mg/mL) by evaporating to dryness in a Petri dish at room temperature.

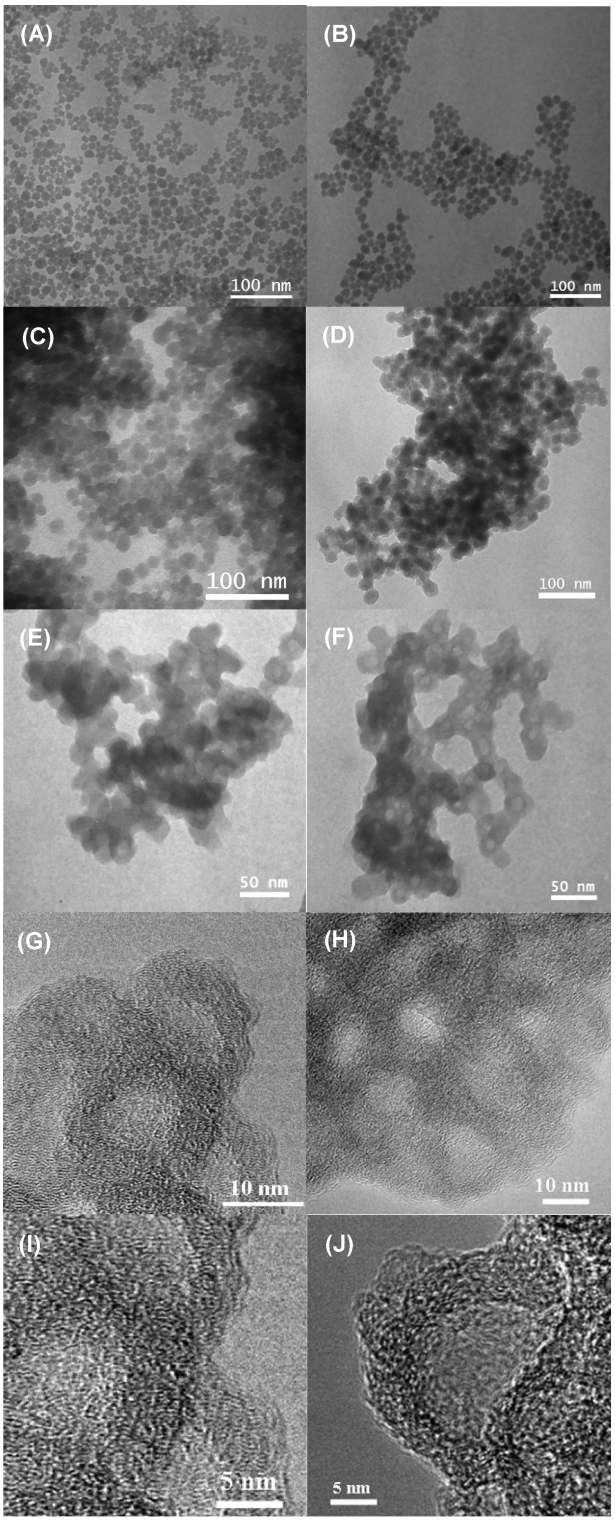

Figure 2. TEM images of (A) SiO_2, (B) SiO_2—Br, (C) SiO_2-*g*-PS, (D) SiO_2/cross-linked PS composite, (E, G, I) nanoporous polystyrene, and (F, H, J) nanoporous carbon.

Figure 2C shows the TEM image of the scratched SiO_2-*g*-PS films. The SiO_2-*g*-PS nanoparticles in the films retain a well-defined spherical shape with average size of about 18 nm and aggregate with each other in various directions. Such aggregation facilitates the interparticle cross-linking during the subsequent

dx.doi.org/10.1021/ma2013207 |*Macromolecules* 2011, 44, 5846–5849

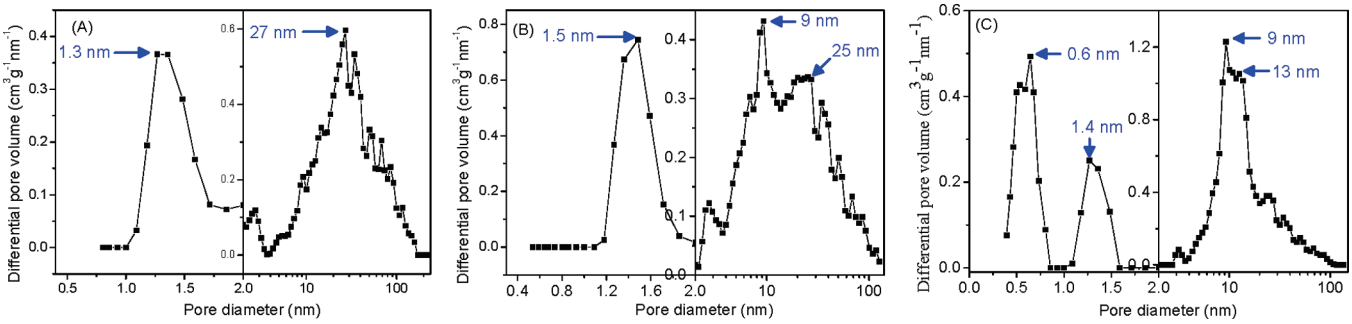

Figure 3. DFT pore size distributions of (A) SiO_2/cross-linked PS composite, (B) nanoporous polystyrene, and (C) nanoporous carbon.

Friedel−Crafts (F−C) reaction. The F−C cross-linking was achieved by placing the SiO_2-*g*-PS films into a heated (75 °C) mixture of anhydrous aluminum chloride and carbon tetrachloride (CCl_4) for 20 h under stirring. The PS chains in the SiO_2-*g*-PS nanoparticles underwent an intraparticle cross-linking process by formation of $-CCl_2-$ cross-linking bridges between the phenyl rings, while swollen in CCl_4. This procedure subdivided the original solid PS shell into numerous micropores because of the formation of a network structure. The $-CCl_2-$ cross-linking bridges were subsequently converted into the −CO− ones by hydrolysis in the presence of water.[3a,d,6] Such −CO− bridges are essential for efficient carbonization of the PS framework and inheritability of the nanostructure during carbonization.[3a,d] Because of the introduction of the cross-linking bridges, the PS shell had a weight gain of about 6%, which translated into the molar ratio of styrene unit to −CO− bridge approximately equal to 4:1. The presence of the resultant micropores was confirmed by an adsorption uptake at low relative pressure in the N_2 adsorption−desorption isotherm of Figure S3.[7] According to the pore size distribution (PSD) curve by density functional theory (DFT),[8] in Figure 3A, the size of the micropores is centered at 1.3 nm. During the cross-linking reaction, the swollen PS chains on the periphery of the shell of the interaggregated nanoparticles in the films could interpenetrate and then be joined with each other by interparticle cross-linking under stirring, eventually leading to the formation of a 3D nanonetwork structure (Figure 2D). Such a nanonetwork contains many mesopores and macropores as a consequence of the combination of compact and loose cross-linked-aggregation of nanoparticles, respectively. The PSD curve, shown in Figure 3A, indicates that the size of these meso-/macropores throughout the 3D network for the as-obtained SiO_2/cross-linked PS composite ranges from 2 to 170 nm with a maximum at 27 nm.

The SiO_2 core was then removed to form a spherical mesopore by treating the SiO_2/cross-linked PS composite with HF, resulting in a totally new targeted network unit. As shown in the TEM images of the as-prepared nanoporous polystyrene, in Figure 2E,G, the network units are well-defined hollow nanospheres, with $d \sim 18$ nm, with a mesosized core and a microporous shell. These units are interconnected with each other in various directions to form a unique 3D meso-/macroporous network structure. A high magnification TEM image, Figure 2I, confirms that the micropores are within a network of cross-linked shells and are 3D interconnected with each other. Additionally, the silica-templated mesoporous cores are separated by cross-linked PS shells. However, since this shell itself is a 3D microporous network, the hierarchical nanopores, including mesoporous core, microporous shell, and meso-/macropores formed in the interparticle network, are interconnected in various directions. Thus, the resulting nanoporous polystyrene has good pore interconnectivity, which is essential in potential applications of these hierarchically porous nanostructured materials.[3b,c] Furthermore, by comparing the PSD curves of the samples before and after etching, Figure 3A vs 3B, the peak at 9 nm can be ascribed to the SiO_2-templating mesosized cores, with the intraparticle network micropores and the interparticle network meso-/macropores concentrated at 1.5 and 25 nm, respectively. The diameter of the SiO_2-templating mesosized cores obtained by the DFT method is slightly lower than that of SiO_2 nanoparticle based on TEM image in Figure 2A, which is most likely due to different characterization principles. The application of Brunauer−Emmett−Teller (BET) equation to the N_2 adsorption−desorption isotherm shown in Figure S3 gives the BET surface area of the nanoporous polystyrene equal to 417 $m^2\ g^{-1}$, and the *t*-plot method gives the corresponding micropore and external, i.e., meso- and macropore, surface areas equal to 143 and 274 $m^2\ g^{-1}$, respectively.

Finally, the targeted nanoporous carbon was obtained by carbonization of the SiO_2/cross-linked PS composite over 3 h at 800 °C (38 wt % of carbonization yield for cross-linked PS shells), followed by etching the resulting SiO_2/carbon composite. A comparison of TEM images of the samples before and after carbonization (Figures 2E,G,I vs 2F,H,J) clearly demonstrates that the carbonyl-cross-linked PS shells retained stability during carbonization, which resulted in a carbon network unit with a mesosized core and a microporous shell structure. However, as in the case of the formation of most porous carbon materials, the initial network framework underwent a certain level of framework shrinkage during the transformation from polymer to carbon because of the loss of many noncarbon elements and carbon-containing compounds during carbonization process.[3a,4c,9] This led to a decrease in the size of interparticle network nanopores from the original 25 to 13 nm; see the comparison of Figures 3B and 3C. Moreover, carbonization led to the formation of numerous new micropores of 0.6 nm in the carbon framework (Figure 3C) which increased the number of micropores, judging from a higher N_2 uptake at low relative pressure (Figure S3). However, the original intraparticle network micropores of 1.4 nm and the SiO_2-templated mesopores of 9 nm were retained after carbonization (Figure 3C). The BET surface area of the as-prepared nanoporous carbon was calculated to be 525 $m^2\ g^{-1}$. The *t*-plot method demonstrated that the micropore surface area and meso-/macropore surface area were 252 and 273 $m^2\ g^{-1}$, respectively. The ratios of micropore (P_{mic}) and meso-/macropore (P_{ext}) to the total surface area were calculated to be 48% and 52%, respectively, according to the following equations: $P_{mic} = (S_{mic}/S_{BET}) \times 100\%$, and $P_{ext} = 100\% - P_{mic}$.

dx.doi.org/10.1021/ma2013207 |*Macromolecules* 2011, 44, 5846–5849

In conclusion, novel NPN polymer and carbon materials with a unique core−shell nanosphere network unit were successfully synthesized by carbonyl-cross-linking of PS chains tethered on silica nanoparticles prepared by SI-ATRP, followed by carbonization. The procedure allowed for the formation of various types of interconnected nanopores: (i) micropores resulting from the intraparticle cross-linking of PS shells, (ii) mesopores formed by removal of silica cores, and (iii) network of meso-/macropores induced by interparticle cross-linking. It is envisioned that further tuning of nanostructures prepared according to this method could be accomplished by variation of silica particle size, molecular weight of PS, grafting density, and cross-linking density. Novel nanoporous materials of this kind hold considerable promise in applications as electrode materials in supercapacitors and fuel cells, as controlled drug delivery systems, advanced catalyst supports, CO_2 capture materials, and as HPLC packing materials.

■ ASSOCIATED CONTENT

Supporting Information. Experimental details, GPC trace, thermogravimetric curve, and N_2 adsorption−desorption isotherms. This material is available free of charge via the Internet at http://pubs.acs.org.

■ AUTHOR INFORMATION

Corresponding Author

*E-mail: km3b@andrew.cmu.edu (K.M.); tomek@andrew.cmu.edu (T.K.); jaroniec@kent.edu (M.J.); wudc@mail.sysu.edu.cn (D.W.).

■ ACKNOWLEDGMENT

We acknowledge financial support from National Science Foundation (DMR 09-69301 and CTS 03-04568). Dr. Wu acknowledges financial support from the project of NNSFC (50802116), SRFDP (200805581014), and the Fundamental Research Funds for the Central Universities (09lgpy18).

■ REFERENCES

(1) (a) Liu, C.; Li, F.; Ma, L.-P.; Cheng, H.-M. *Adv. Mater.* **2010**, *22*, E28. (b) Su, D. S.; Schlögl, R. *ChemSusChem* **2010**, *3*, 136. (c) Titirici, M.-M.; Antonietti, M. *Chem. Soc. Rev.* **2010**, *39*, 103. (d) Lee, J.; Kim, J.; Hyeon, T. *Adv. Mater.* **2006**, *18*, 2073. (e) White, R. J.; Tauer, K.; Antonietti, M.; Titirici, M.-M. *J. Am. Chem. Soc.* **2010**, *132*, 17360. (f) Bang, J.; Jeong, U.; Ryu, D. Y.; Russell, T. P.; Hawker, C. J. *Adv. Mater.* **2009**, 4769. (g) Wu, D.; Li, Z.; Liang, Y.; Yang, X.; Zeng, X.; Fu, R. *Carbon* **2009**, *47*, 916.

(2) (a) Xu, Z.; Zhang, W.; Lv, L.; Pan, B.; Lan, P.; Zhang, Q. *Environ. Sci. Technol.* **2010**, *44*, 3130. (b) Chen, Z.; Zhang, A.; Li, J.; Dong, F.; Di, D.; Wu, Y. *J. Phys. Chem. B* **2010**, 4841. (c) Yang, S. Y.; Ryu, I.; Kim, H. Y.; Kim, J. K.; Jang, S. K.; Russell, T. P. *Adv. Mater.* **2006**, *18*, 709. (d) Zhu, F.; Guo, J.; Zeng, F.; Fu, R.; Wu, D.; Luan, T.; Tong, Y.; Lu, T.; Ouyang, G. *J. Chromatogr., A* **2010**, *1217*, 7848. (e) Song, S.; Liang, Y.; Li, Z.; Wang, Y.; Fu, R.; Wu, D.; Tsiakaras, P. *Appl. Catal., B* **2010**, *98*, 132. (f) Liang, Y.; Liang, F.; Li, Z.; Wu, D.; Yan, F.; Li, S.; Fu, R. *Phys. Chem. Chem. Phys.* **2010**, *12*, 10842. (g) Song, S.; Yin, S.; Li, Z.; Shen, P. K.; Fu, R.; Wu, D. *J. Power Sources* **2010**, *195*, 1946. (h) Yang, X.; Wu, D.; Chen, X.; Fu, R. *J. Phys. Chem. C* **2010**, *114*, 8581. (i) Dresselhaus, M. S. *Annu. Rev. Mater. Sci.* **1997**, *27*, 1. (j) Wang, J.; Yang, X.; Wu, D.; Fu, R.; Dresselhaus, M. S.; Dresselhaus, G. *J. Power Sources* **2008**, *185*, 589. (k) Wu, X.; Yang, X.; Wu, D.; Fu, R. *Chem. Eng. J.* **2008**, *138*, 47. (l) Wu, X.; Wu, D.; Fu, R. *J. Hazard. Mater.* **2007**, *147*, 1028.

(3) (a) Zou, C.; Wu, D.; Li, M.; Zeng, Q.; Xu, F.; Huang, Z.; Fu, R. *J. Mater. Chem.* **2010**, *20*, 731. (b) Wang, D.-W.; Li, F.; Liu, M.; Lu, G. Q.; Cheng, H.-M. *Angew. Chem., Int. Ed.* **2008**, *47*, 373. (c) Xu, F.; Cai, R.; Zeng, Q.; Zou, C.; Wu, D.; Li, F.; Lu, X.; Liang, Y.; Fu, R. *J. Mater. Chem.* **2011**, *21*, 1970. (d) Zeng, Q.; Wu, D.; Zou, C.; Xu, F.; Fu, R.; Li, Z.; Liang, Y.; Su, D. *Chem. Commun.* **2010**, *46*, 5927.

(4) (a) Al-Muhtaseb, S. A.; Ritter, J. A. *Adv. Mater.* **2003**, *15*, 101. (b) Wu, D.; Fu, R.; Dresselhaus, M. S.; Dresselhaus, G. *Carbon* **2006**, *44*, 675. (c) Wu, D.; Fu, R.; Zhang, S.; Dresselhaus, M. S.; Dresselhaus, G. *Carbon* **2004**, *42*, 2033.

(5) (a) Pyun, J.; Jia, S.; Kowalewski, T.; Patterson, G. D.; Matyjaszewski, K. *Macromolecules* **2003**, *36*, 5094. (b) Bombalski, L.; Dong, H.; Listak, J.; Matyjaszewski, K.; Bockstaller, M. R. *Adv. Mater.* **2007**, *19*, 4486. (c) Choi, J.; Dong, H.; Matyjaszewski, K.; Bockstaller, M. R. *J. Am. Chem. Soc.* **2010**, *132*, 12537. (d) Wang, J. S.; Matyjaszewski, K. *J. Am. Chem. Soc.* **1995**, *117*, 5614. (e) Matyjaszewski, K.; Tsarevsky, N. V. *Nature Chem.* **2009**, *1*, 276. (f) Wu, D.; Dong, H.; Pietrasik, J.; Kim, E. K.; Hui, C.; Zhong, M.; Jaroniec, M.; Kowalewski, T.; Matyjaszewski, K. *Chem. Mater.* **2011**, *23*, 2024.

(6) Hradil, J.; Králová, E. *Polymer* **1998**, *39*, 6041.

(7) Gregg, S. J.; Sing, K. S. W. *Adsorption, Surface Area and Porosity*; Academic Press: New York, 1982.

(8) (a) Jagiello, J.; Olivier, J. P. *J. Phys. Chem. C* **2009**, *113*, 19382. (b) Lastoskie, C.; Gubbins, K. E.; Quirke, N. *Langmuir* **1993**, *9*, 2693. (c) Ravikovitch, P. I.; Vishnyakov, A.; Russo, R.; Neimark, A. V. *Langmuir* **2000**, *16*, 2311. (d) Jagiello, J.; Thommes, M. *Carbon* **2004**, *42*, 1227. (e) Neimark, A. V.; Ravikovitch, P. I.; Grün, M.; Schüth, F.; Unger, K. K. *J. Colloid Interface Sci.* **1998**, *207*, 159.

(9) (a) Wu, D.; Fu, R. *J. Porous Mater.* **2005**, *12*, 311. (b) Wu, D.; Fu, R.; Yu, Z. *J. Appl. Polym. Sci.* **2005**, *96*, 1429.